Fast and effective extraction
for equivalent shunt resistances
of triple-junction concentrator solar cells

HUI LV[1, 2*], JINMEI DAI[1, 2], FEI SHENG[1, 2], WEN LIU[1, 3],
XINGUO MA[1, 2], CHUNFU CHENG[1, 2], QINGHUA LV[1, 2]

[1]Hubei Collaborative Innovation Center for High-efficiency Utilization of Solar Energy,
 Hubei University of Technology, Wuhan 430068, P.R. China

[2]School of Science, Hubei University of Technology, Wuhan 430068, P.R. China

[3]Institute of Advanced Technology, University of Science and Technology of China,
 Hefei 230022, P.R. China

*Corresponding author: simonlv76@gmail.com

Fast and effective extraction of equivalent shunt resistance for each subcell of GaInP/GaInAs/Ge triple-junction concentrator solar cells is presented. The two-diode model of single junction was introduced to establish the equivalent circuit of triple-junction solar cells. The current-voltage characteristic of the triple-junction solar cells was measured under AM1.5D spectrum, $C = 576$ and $T = 303$ K. Equivalent shunt resistance of each subcell was extracted from its estimated current-voltage curve. The estimated current-voltage curve of the triple-junction solar cells shows a good agreement with the experimental data in 0.31% deviation. The degradation in the equivalent shunt resistance for Ge subcell was intentionally introduced to indicate the mechanism of current--matching operation for different subcells, with the maximum output power of the triple-junction solar cells deteriorating from 3.5 to 3.17 W. The results can offer performance analysis and optimum design of photovoltaic applications.

Keywords: concentrator photovoltaic, triple-junction solar cell, equivalent shunt resistance.

1. Introduction

Multi-junction concentrator solar cells have been developed as a promising solution for photovoltaic applications [1]. At present, triple-junction solar cells (TJSC) have reached an efficiency of 44.4% at 302 suns [2]. Equivalent shunt resistance is a lumped component to describe the alternative paths for the current flow through the inherent diode or along the cell edges, characterizing the leak current in a solar cell [3]. This parameter is caused by defects such as lattice imperfections or doping concentration ratio in/near the depletion region, and *p-n* junction penetration [4, 5].

Since the subcells are electrically connected in series, the TJSC current is limited by the subcell that produces the lowest current. At the zero-biased (short-circuit) con-

dition, the current-limiting behavior drives the subcell of lower shunt resistance into negative bias while the other two under positive bias, thus the voltage of the TJSC exhibits the zero voltage or zero bias [6]. The subcell under negative bias acts as a load, consuming the power generated by other subcells [7]. Large leak current is undesirably derived and entails performance degradation of the TJSC due to the power loss. Besides, for each subcell, the higher equivalent shunt resistance, the higher fill factor and efficiency, and the better output characteristic [8]. Thus, accurate evaluation of equivalent shunt resistance is required to improve the TJSC performance.

Several approaches are proposed in literatures for current-voltage (*I-V*) characteristics measurement of solar cells, based on the single-diode model and the two-diode model [9–11]. The Lambert *W* function has been applied to investigate properties of the TJSC [9]. This numerical extraction achieves explicit analytic expression of *I-V* by the conventional single-diode model. A straightforward method was developed to quantify the equivalent shunt resistance of a selected solar cell of a photovoltaic module, which depends on the *I-V* characteristic measurement of the installed cell string when intentionally shading the selected cell [10]. As reported recently, the self-consistent iteration has been introduced to obtain electrical parameters by fitting the experimental bias voltage-dependent spectral response of GaInP/GaInAs/Ge TJSC [11]. However, practical difficulties may be faced when the *I-V* characteristic of the selected cell are evaluated under different monochromatic light wavelengths, illumination levels (even in dark).

In this paper, equivalent shunt resistance for each subcell of $Ga_{0.35}In_{0.65}P/Ga_{0.83}In_{0.17}As/Ge$ concentrator solar cells is extracted by mathematical iterations. A precise expression of *I-V* is obtained from the coupled two-diode *I-V* characteristic transcend formula, in which shunt resistance for each subcell is regarded as infinity. Electrical parameters are also derived from the measured *I-V* characteristic of the TJSC. Additionally, performance degradation of the TJSC is discussed when the equivalent shunt resistance decrease for Ge subcell is intentionally deteriorated.

2. Theory

The lumped equivalent circuit model for a GaInP/GaInAs/Ge TJSC is shown in Fig. 1. Each subcell is viewed as a *p-n* junction with two diodes, which represents recombination in the quasi-neutral and the depletion regions, respectively.

The *I-V* relation for the TJSC is given by

$$I = I_{sci} - I_{o1i}\left[\exp\frac{q(V_i + IR_{si})}{k_B T} - 1\right] - I_{o2i}\left[\exp\frac{q(V_i + IR_{si})}{2k_B T} - 1\right] - \frac{V_i + IR_{si}}{R_{shi}} \quad (1)$$

where *i* represents the subcell number (1 – top, 2 – middle and 3 – bottom); *I* is the load current and I_{sci} is the short-circuit current (approximately equal to the photo-generated current [12]); I_{o1i} or I_{o2i} is the reverse dark saturation current for each diode; R_{si} and R_{shi} are the series and the shunt resistances, respectively; *q*, V_i, k_B and *T* is
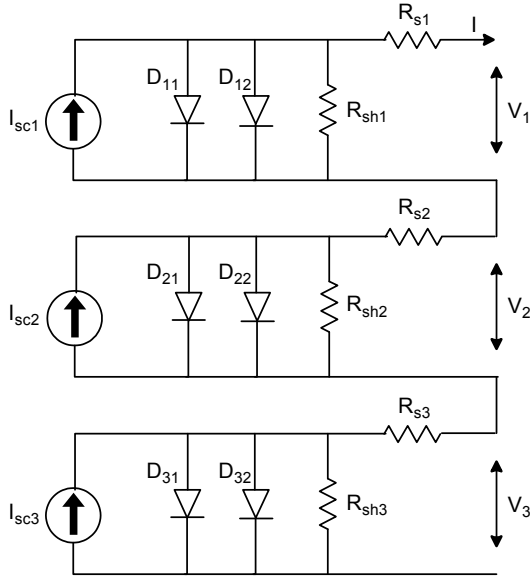
Fig. 1. Equivalent circuit with two-diode model for the TJSC.

the electric charge, the single-junction voltage, Boltzmann's constant, the absolute temperature, respectively. Number 1 or 2 fixed in the exponent function is the diode ideality factor. The terminal voltage is given by the sum of voltages of three serried--connected subcells

$$V = V_1 + V_2 + V_3 \tag{2}$$

The model implies a strong dependence on temperature as follows [13]:

$$I_{o1i} = S\kappa_{1i}T^3 \exp\left(-\frac{E_{gi}}{k_B T}\right) \tag{3}$$

$$I_{o2i} = S\kappa_{2i}T^{5/2} \exp\left(-\frac{E_{gi}}{2k_B T}\right) \tag{4}$$

$$E_g = E_g\big|_{T=0} - \frac{\alpha T^2}{T+\beta} \tag{5}$$

where κ_{1i} and κ_{2i} are constants of each subcell obtained by fitting the measured *I-V* curve of the TJSC; *S* is the active area of the TJSC and E_{gi} is the energy band gap of each subcell. For semiconductors' alloy composition ($A_{1-x}B_x$), E_g is determined by [14]

$$E_g(A_{1-x}B_x) = (1-x)E_g(A) + xE_g(B) - x(1-x)P \tag{6}$$

where *P* is an alloy ingredients dependent parameter for the semiconductor alloy.

If $R_{shi} \to \infty$, the last term in Eq. (1) can be neglected. Equation (1) is rearranged as follows:

$$I_{o1i}\left[\exp\frac{q(V_i + IR_{si})}{2k_BT}\right]^2 + I_{o2i}\left[\exp\frac{q(V_i + IR_{si})}{2k_BT}\right] + I - (I_{sci} + I_{o1i} + I_{o2i}) = 0 \tag{7}$$

$$I_{o1i}X^2 + I_{o2i}X + I - (I_{sci} + I_{o1i} + I_{o2i}) = 0 \tag{8}$$

where

$$X = \exp\frac{q(V_i + IR_{si})}{2k_BT} \tag{9}$$

The positive root can be solved from Eq. (8) as

$$X = \frac{\sqrt{I_{o2i}^2 - 4I_{o1i}[I - (I_{sci} + I_{o1i} + I_{o2i})]} - I_{o2i}}{2I_{o1i}} \tag{10}$$

The single-junction voltage and the overall voltage of the TJSC are written as:

$$V_i = \frac{2k_BT}{q}\ln\frac{\sqrt{I_{o2i}^2 - 4I_{o1i}[I - (I_{sci} + I_{o1i} + I_{o2i})]} - I_{o2i}}{2I_{o1i}} - IR_{si} \tag{11}$$

$$V = \frac{2k_BT}{q}\sum_{i=1}^{3}\ln\frac{\sqrt{I_{o2i}^2 - 4I_{o1i}[I - (I_{sci} + I_{o1i} + I_{o2i})]} - I_{o2i}}{2I_{o1i}} - IR_s \tag{12}$$

where the total series resistance $R_s = R_{s1} + R_{s2} + R_{s3}$. The average error e_{ave} and the root mean square (RMS) error are defined as:

$$e_{ave} = \frac{1}{N}\sum_{m=1}^{N}(V_m - V_m') \tag{13}$$

$$\text{RMS} = \sqrt{\frac{1}{N}\sum_{m=1}^{N}\left(\frac{V_m - V_m'}{V_m}\right)^2} \tag{14}$$

3. Extraction algorithm

3.1. Input parameters

In this work, both uniform illumination and a concentration ratio of 576 ($C = 576$, according to the real design of concentrator optics and solar cell) are assumed. Under
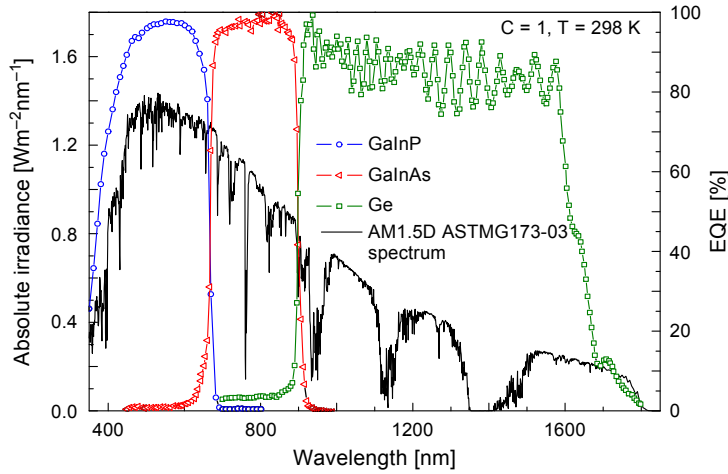
Fig. 2. AM1.5D ASTM G173-03 spectrum and EQE at $C = 1$ and $T = 298$ K.

T a b l e 1. Input parameters of the TJSC ($S = 5.5 \times 5.5$ cm^2).

	GaP	InP	GaAs	InAs	Ge
$E_g(T = 0$ K) [eV]	2.86	1.41	1.52	0.42	0.74
$\alpha \times 10^4$ [eV^{-1}K^{-1}]	5.77	3.63	5.41	4.19	4.77
β [K]	371	162	204	271	235
Alloy composition	Ga$_{0.35}$In$_{0.65}$P		Ga$_{0.83}$In$_{0.17}$As		Ge
P [eV]	0.64		0.30		–
$E_{gi}(T = 298$ K) [eV]	1.70		1.20		0.66
$I_{sci}(C = 576, T = 298$ K) [mA]	2.32		2.31		2.90

AM1.5D ASTM G173-03 standard spectrum at $C = 1$ and $T = 298$ K, the subcell short-circuit current was calculated from external quantum efficiency (EQE) in the TJSC manufacturers' datasheet [15] (as shown in Fig. 2). Input parameters of the TJSC are given in Table 1 [16]. Concentration ratio and temperature dependence of the subcell short-circuit current are defined as:

$$ I_{sci}\big|_{C = 576, T} = I_{sci}\big|_{C = 576, T = 298} + \frac{\mathrm{d}I_{sci}}{\mathrm{d}T}\bigg|_{C = 576, T} \times (T - 298) \tag{15} $$

3.2. Extraction algorithm

Shunt resistance for each subcell is related to the slope at the short-circuit point of its *I-V* curve. The adopted iterative algorithm is described in the following steps:

   0) Consider an initial set ($R_{shi} \to \infty$) in Eq. (1). Parameters of κ_{1i}, κ_{2i}, $\mathrm{d}I_{sci}/\mathrm{d}T$ and R_{si} are extracted by fitting the measured *I-V* curve of the TJSC using Eq. (12). These parameters are suitable for considerable temperature and concentration ratio.

1) Determine the operational point ($I = 0$, $V_i = V_{opi}$) and the short-circuit current ($I = I_{sci}$, $V_i = 0$) of each subcell. Assuming all the subcells are working at the measured short-circuit current point of the TJSC ($I = I_{sc}$, $V = 0$), V_{opi} is evaluated using Eq. (1). I_{sci} is obtained from Eq. (15).

2) Calculate new values of R_{shi} in Eq. (1). These values are derived from the slope of the two points in step 2 by $R_{shi} = |\Delta V_i / \Delta I_i| = |(0 - V_{opi})/(I_{sci} - 0)|$.

3) Repeat steps 1 and 2 with mathematical iterations. R_{shi} are obtained when the difference between consecutive iteration is below 10^{-3}.

4. Results and discussion

The unknown parameters in the model are extracted by fitting the measured *I-V* curve of the TJSC at $C = 576$ and $T = 303$ K, as listed in Table 2. RMS = 0.31% and $e_{ave} = 0.001$ V show a good agreement. The measured and estimated results of the TJSC and each subcell are plotted in Fig. 3. The estimated maximum power of the TJSC ($P'_{max} = 3.492$ W) is very close to the measured ($P_{max} = 3.495$ W). Shunt resistances of the three subcells are extracted as 27242, 2531 and 345 Ω, respectively. As shown in Fig. 3, the terminal current of the TJSC is limited by the GaInAs subcell. The short-circuit current of the Ge subcell is the highest. However, the excess generated current of Ge subcell is wasted by thermalization at the short-circuit condition.

T a b l e 2. Extracted parameters of the TJSC.

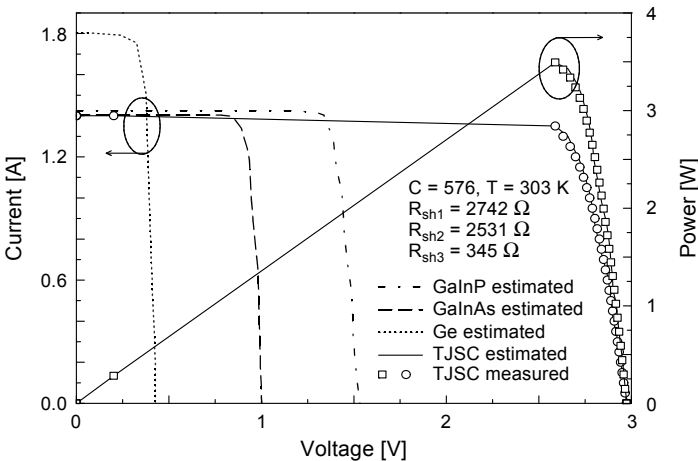| Subcell	$Ga_{0.35}In_{0.65}P$	$Ga_{0.83}In_{0.17}As$	Ge
$\kappa_{1i} \times 10^3$ [Am^{-2}]	0.43	0.85	15.72
$\kappa_{2i} \times 10^3$ [Am^{-2}]	28.21	36.19	1.44
dI_{sci}/dT (C = 576) [mV·K^{-1}]	2.42	2.42	1.81
R_{si} [Ω]	0.045	0.035	0.025

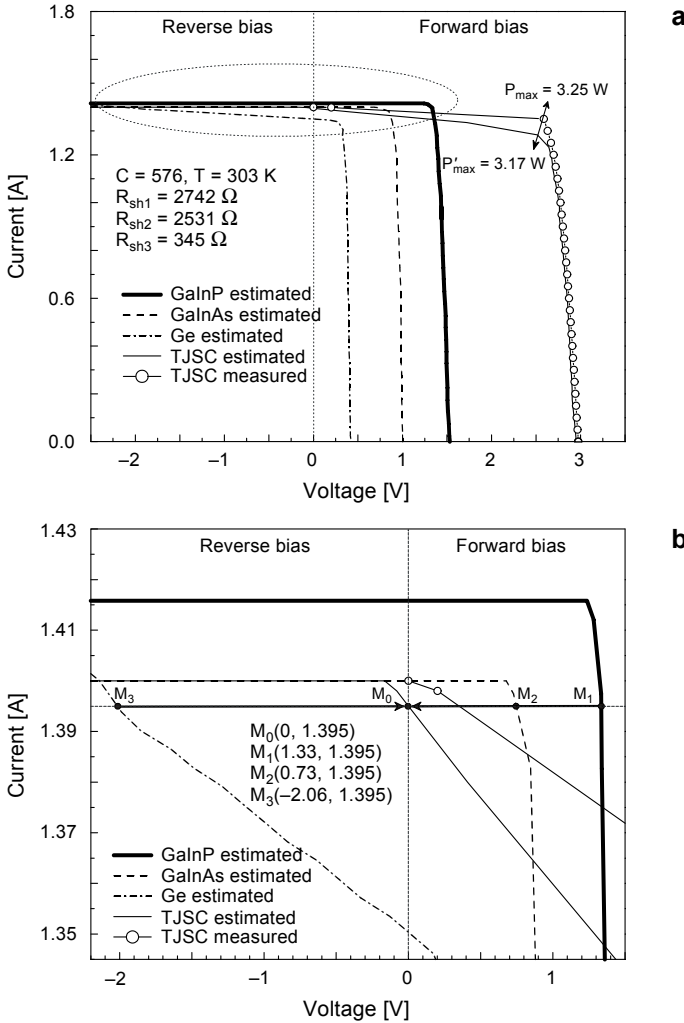Fig. 3. Measured and estimated results of TJSC and each subcell (*I-V* and power curves).

Fig. 4. *I-V* curves with deliberate decrease in shunt resistance for Ge subcell – **a**. The close up of the difference in (**a**) – **b**.

In order to better understand performance degradation of the TJSC, the shunt resistance of Ge subcell was intentionally decreased from 345 to 45 Ω (approximately one order of magnitude lower), as illustrated in Fig. 4**a**. The short-circuit current of the Ge subcell shifts from 1.80 A (in the previous estimation) to 1.35 A. For the deteriorated situation, P'_{max} drops to 3.17 W, much lower than P_{max}. In practice, defects introduced in the epitaxial process for semiconductor devices may produce reduction of the shunt resistances for the TJSC. Reverse leak current of the Ge subcell increases as its shunt resistance decreases. Part of its photo-generated current is used to overcome the leak current. These can be clearly illustrated as in Fig. 4**b**, as the close up of the circled area in Fig. 4**a**. The TJSC and each subcell at their respective operating

point correspond to M_0, M_1, M_2 and M_3 in Fig. **4b**. The mechanism of current-matching operation drives the Ge subcell to a reverse-biased state, in order to meet the short--circuit condition of the TJSC (TJSC voltage of 0 V = 1.33 V + 0.73 V − 2.06 V). In this case, the shunt resistance of the Ge subcell should be taken into account due to the fact that the reverse leak current occurring in the Ge subcell is not negligible.

5. Conclusions

Fast and effective extraction for equivalent shunt resistance of each subcell of $Ga_{0.35}In_{0.65}P/Ga_{0.83}In_{0.17}As/Ge$ concentrator solar cells was proposed. Based on the two-diode model, this extraction was calibrated by the experimental *I-V* characteristic of the TJSC under determined flux concentration and temperature. Shunt resistance of each subcell was extracted from the slope of its estimated *I-V* curve by mathematical iterations. Extracted results of the shunt resistances were obtained as 27242 Ω for the top subcell, 2531 Ω for the middle subcell and 345 Ω for the bottom subcell. Furthermore, a deliberate decrease in shunt resistance for the Ge subcell was performed. In this situation, serious power loss and performance degradation of the TJSC are estimated. The iterative method proposed in this paper can be applied to extract equivalent shunt resistance for all series-connected multi-junction solar cells. The results can also offer performance analysis and optimum design of solar cells.

References

[1] KOZŁOWSKA A., NAKIELSKA M., SARNECKI J., LIPIŃSKA L., JEREMIASZ O., PODNIESIŃSKI D., MALĄG A., *Spectroscopic investigations of rare-earth materials for luminescent solar concentrators*, Optica Applicata **41**(2), 2011, pp. 359–365.

[2] GREEN M.A., EMERY K., HISHIKAWA Y., WARTA W., DUNLOP E.D., *Solar cell efficiency tables (version 43)*, Progress in Photovoltaics: Research and Applications **22**(1), 2014, pp. 1–9.

[3] ASAF BEN OR, APPELBAUM J., *Estimation of multi-junction solar cell parameters*, Progress in Photovoltaics: Research and Applications **21**(4), 2013, pp. 713–723.

[4] ZHANG LUCHENG, SHEN HUI, *Novel approach for characterizing the specific shunt resistance caused by the penetration of the front contact through the p–n junction in solar cell*, Journal of Semiconductors **30**(7), 2009, article 074007.

[5] PRAŻMOWSKA J., PASZKIEWICZ R., KORBUTOWICZ R., WOŚKO M., TŁACZAŁA M., *Solar cells conversion efficiency enhancement techniques*, Optica Applicata **37**(1–2), 2007, pp. 93–98.

[6] SOGABE T., OGURA A., OKADA Y., *Analysis of bias voltage dependent spectral response in $Ga_{0.51}In_{0.49}P/Ga_{0.99}In_{0.01}As/Ge$ triple junction solar cell*, Journal of Applied Physics **115**(7), 2014, article 074503.

[7] PARASKEVA V., HADJIPANAYI M., NORTON M., PRAVETTONI M., GEORGHIOU G.E., *Voltage and light bias dependent quantum efficiency measurements of GaInP/GaInAs/Ge triple junction devices*, Solar Energy Materials and Solar Cells **116**, 2013, pp. 55–60.

[8] GIAFFREDA D., MAGNONE P., MENEGHINI M., BARBATO M., MENEGHESSO G., ZANONI E., SANGIORGI E., FIEGNA C., *Local shunting in multicrystalline silicon solar cells: distributed electrical simulations and experiments*, IEEE Journal of Photovoltaics **4**(1), 2014, pp. 40–47.

[9] NAOREM SANTAKRUS SINGH, AVINASHI KAPOOR, *Determining multi-junction solar cell parameters using Lambert-W function*, Paripex – Indian Journal of Research **3**(5), 2014, pp. 203–206.

[10] D'ALESSANDRO V., GUERRIERO P., DALIENTO S., GARGIULO M., *A straightforward method to extract the shunt resistance of photovoltaic cells from current-voltage characteristics of mounted arrays*, Solid-State Electronics **63**(1), 2011, pp. 130–136.

[11] SOGABE T., OGURA A., OHBA M., OKADA Y., *Self-consistent electrical parameter extraction from bias dependent spectral response measurements of III-V multi-junction solar cells*, Progress in Photovoltaics: Research and Applications **23**(1), 2015, pp. 37–48.

[12] SWEE HOE LIM, JING-JING LI, STEENBERGEN E.H., YONG-HANG ZHANG, *Luminescence coupling effects on multijunction solar cell external quantum efficiency measurement*, Progress in Photovoltaics: Research and Applications **21**(3), 2013, pp. 344–350.

[13] KINSEY G.S., EDMONDSON K.M., *Spectral response and energy output of concentrator multijunction solar cells*, Progress in Photovoltaics: Research and Applications **17**(5), 2009, pp. 279–288.

[14] VURGAFTMAN I., MEYER J.R., RAM-MOHAN L.R., *Band parameters for III-V compound semiconductors and their alloys*, Journal of Applied Physics **89**(11), 2001, pp. 5815–5875.

[15] http://www.azurspace.com/images/products/DB_3988-00-00_3C42_AzurDesign_EFA_55x55_2014-03-27.pdf

[16] SEGEV G., MITTELMAN G., KRIBUS A., *Equivalent circuit models for triple-junction concentrator solar cells*, Solar Energy Materials and Solar Cells **98**, 2012, pp. 57–65.